Original Article | Neuroimaging and Head & Neck

eISSN 2005-8330
https://doi.org/10.3348/kjr.2020.0178
Korean J Radiol 2021;22(7):1142-1151

Check for updates

Korean Journal of Radiology
KJR

Characterization of Brain Microstructural Abnormalities in High Myopia Patients: A Preliminary Diffusion Kurtosis Imaging Study

Huihui Wang[1], Hongwei Wen[2], Jing Li[1], Qian Chen[1], Shanshan Li[1], Yanling Wang[3], Zhenchang Wang[1]

Departments of [1]Radiology and [3]Ophthalmology, Beijing Friendship Hospital, Capital Medical University, Beijing, China; [2]Key Laboratory of Cognition and Personality (Ministry of Education), School of Psychology, Southwest University, Chongqing, China

Objective: To evaluate microstructural damage in high myopia (HM) patients using 3T diffusion kurtosis imaging (DKI).
Materials and Methods: This prospective study included 30 HM patients and 33 age- and sex-matched healthy controls (HCs) with DKI. Kurtosis parameters including kurtosis fractional anisotropy (FA), mean kurtosis (MK), axial kurtosis (AK), and radial kurtosis (RK) as well as diffusion metrics including FA, mean diffusivity, axial diffusivity (AD), and radial diffusivity derived from DKI were obtained. Group differences in these metrics were compared using tract-based spatial statistics. Partial correlation analysis was used to evaluate correlations between microstructural changes and disease duration.
Results: Compared to HCs, HM patients showed significantly reduced AK, RK, MK, and FA and significantly increased AD, predominately in the bilateral corticospinal tract, right inferior longitudinal fasciculus, superior longitudinal fasciculus, inferior fronto-occipital fasciculus, and left thalamus (all $p < 0.05$, threshold-free cluster enhancement corrected). In addition, DKI-derived kurtosis parameters (AK, RK, and MK) had negative correlations ($r = -0.448$ to -0.376, all $p < 0.05$) and diffusion parameter (AD) had positive correlations ($r = 0.372$ to 0.409, all $p < 0.05$) with disease duration.
Conclusion: HM patients showed microstructural alterations in the brain regions responsible for motor conduction and vision-related functions. DKI is useful for detecting white matter abnormalities in HM patients, which might be helpful for exploring and monitoring the pathogenesis of the disease.
Keywords: *High myopia; Diffusional kurtosis imaging; Brain; White matter*

INTRODUCTION

High myopia (HM) is a common health issue characterized by visual disability, affecting 2.9% of the global population and 10–20% of young adults in East and Southeast Asia [1,2]. HM is defined by an ocular refractive error less than -6.00 diopters (D) or an axial length greater than 26 mm. HM is also known as "pathological myopia" or "degenerative myopia", reflecting the widespread progressive trend toward the development of pathological and degenerative changes in the neurosensory retina and choroid, which may extend to structures of the brain [3,4]. There are a few previous studies that detected alterations in brain volume and white matter (WM) concentrations in HM patients [5,6]. Shu et al. [7] considered that a lack of afferent visual information input may lead to transneuronal degeneration

Received: February 27, 2020 **Revised:** June 28, 2020 **Accepted:** July 17, 2020
This work was supported by the National Natural Science Foundation of China (grant number: 61527807, 81800840, 81701644, 61801311, 81871322), Beijing Scholars Program (grant number: [2015] 160), Beijing Municipal Administration of Hospitals (grant number: SML20150101, PX2018001, YYZZ2017A14, YYZZ2017B01), and Fundamental Research Funds for the Central Universities (SWU118065).
Corresponding author: Zhenchang Wang, MD, Department of Radiology, Beijing Friendship Hospital, Capital Medical University, No.95, Yong'an Rd, Xicheng District, Beijing 100050, China.
• E-mail: cjr.wzhch@vip.163.com
This is an Open Access article distributed under the terms of the Creative Commons Attribution Non-Commercial License (https://creativecommons.org/licenses/by-nc/4.0) which permits unrestricted non-commercial use, distribution, and reproduction in any medium, provided the original work is properly cited.

Copyright © 2021 The Korean Society of Radiology

Korean Journal of Radiology
KJR

and plastic changes in the visual system and other brain systems. However, in contrast to other ophthalmology-related diseases, such as glaucoma, amblyopia, and blindness [8-10], WM alterations in HM have not been thoroughly explored. Therefore, we speculated that long-term visual abnormalities caused by HM are accompanied by microstructural changes in WM, which may be helpful for exploring and monitoring the pathogenesis of the disease.

Diffusion tensor imaging (DTI) is the most used magnetic resonance imaging (MRI) method to provide quantitative measures of microstructural integrity and organization *in vivo*. DTI, which measures water diffusion based on the hypothesis that water molecules move in a Gaussian distribution pattern, has been widely applied to evaluate microstructural abnormalities in the WM of the brain [11]. However, water molecules often show non-Gaussian diffusion in biological tissues due to the presence of barriers, such as organelles and cell membranes. Therefore, the practicality and sensitivity of the DTI model may not be entirely optimal [12]. Diffusional kurtosis imaging (DKI), as a natural extension of the DTI model, enables quantification of non-Gaussian diffusion and can be used to quantify the microstructural integrity and tissue complexity of WM even in the presence of crossing fibers [12,13]. DKI can acquire both diffusion metrics, such as fractional anisotropy (FA), mean diffusivity (MD), axial diffusivity (AD), and radial diffusivity (RD) as well as kurtosis parameters, including kurtosis FA (KFA), mean kurtosis (MK), axial kurtosis (AK), and radial kurtosis (RK), simultaneously by estimating the excess kurtosis of the displacement distribution. Further, it has exhibited improved sensitivity and specificity in assessing developmental and pathological changes in neural tissues compared to conventional DTI [13].

In the present study, we aimed to explore microstructural impairments and assess the performance of the DKI model in detecting WM abnormalities in patients with HM. Moreover, relationships between these indices and disease duration were also analyzed.

MATERIALS AND METHODS

Subjects

This study was approved by the ethics committee of Beijing Friendship Hospital, Capital Medical University, and each subject provided written informed consent before participation in accordance with the Declaration of Helsinki (IRB No. 2019-P2-201-01).

A total of 35 HM patients were recruited from outpatient clinics of Beijing Friendship Hospital, Capital Medical University from January 2017 to December 2018. Thirty-five age- and sex-matched healthy controls (HCs) with uncorrected visual acuity ≥ 1.0 were also recruited. All subjects were right-handed. The exclusion criteria were as follows: any other ocular diseases (e.g., glaucoma, amblyopia, strabismus, and optic neuritis); unilateral HM; psychiatric disorders; cerebral infarction diseases; any systemic diseases that may influence the results, such as diabetes and hypertension; MRI ineligibility (e.g., cardiac pacemaker, replacement heart valves or implanted metal devices); and MR images with visible artifacts, cerebral infarction lesions, brain tumors, or obvious WM hyperintensities. Overall, five HM patients and two HCs were excluded according to the exclusion criteria.

Image Acquisition

All scans were acquired using a Discovery MR 750 3T scanner (GE Healthcare) with an eight-channel, phased-array head coil. Regular T2-weighted fast-spin-echo images were obtained before acquiring diffusion kurtosis images. DKI was acquired with two b values (b = 1000 and 2000 s/mm^2) along 25 diffusion-encoding directions and a b value of 0 s/mm^2 along five non-diffusion-weighted directions using a spin-echo, single-shot, echo-planar imaging sequence with the following parameters: repetition time/echo time = 9000/96 ms; slice thickness = 3.0 mm without a gap; 44 axial slices; matrix = 256 x 256; field of view = 256 x 256 mm; and acquisition time = 8 minutes and 42 seconds.

Data Preprocessing

Eddy current-induced distortion and motion artifacts in the DKI dataset were corrected using an affine alignment of each diffusion-weighted image to the b = 0 images using the FMRIB diffusion toolbox (FSL 4.0, http://www.fmrib.ox.ac.uk/fsl). After skull stripping, the Diffusional Kurtosis Estimator (http://www.nitrc.org/projects/dke) was implemented to calculate the diffusion and kurtosis tensors using the constrained linear least squares-quadratic programming algorithm as previously described [14]. All data (b = 0, 1000, 2000 s/mm^2) were used for DKI fitting. Maps for the following DKI parameters were then generated: KFA, MK, AK, RK, FA, MD, AD, and RD.

https://doi.org/10.3348/kjr.2020.0178

TBSS Analysis

Statistical analysis of the DKI data was performed using tract-based spatial statistics (TBSS) from a part of the FMRIB Software Library (FSL). Extracted brain images were acquired using the Brain Extraction Tool in the FSL. All subjects' DKI-derived FA images were aligned to a template of averaged FA images (FMRIB-58) in the MNI space using a nonlinear registration tool and affine aligned to 1 x 1 x 1 mm^3. After transformation into the MNI space, a mean FA image was created and thinned to generate a mean FA skeleton of the WM tracts. Each subject's FA images was then projected onto the skeleton via filling the mean FA skeleton with FA values from the nearest relevant tract center by searching perpendicular to the local skeleton structure for maximum FA values [15]. The registration and projection information derived from the FA analysis were then applied to the other DKI parametric images of each subject to ensure the exact spatial correspondence of the different parameters (Fig. 1).

Voxel-wise statistical analysis of the skeleton space across subjects was carried out using a permutation-based inference tool for nonparametric statistics (randomize tool). p values < 0.05 were identified as significant and corrected for multiple comparisons with the threshold-free cluster enhancement (TFCE) method [16] to avoid the definition of an initial cluster-forming threshold and extensive data smoothing. Significant clusters (with their sizes and MNI coordinates of the maximum intensity voxel) were identified using the cluster command tool in the FSL, and fiber tracts corresponding to the clusters were identified using the ICBM-DTI-81 White matter labels atlas, JHU White Matter Tractography Atlas, and Talairach Daemon Labels Atlas. The percentage of abnormal voxels relative to voxels of the whole skeleton was calculated for each parameter to quantitatively compare the sensitivity of parameters derived from DKI in detecting brain tissue integrity impairments in patients with HM.

The Operating System and computer specifications for performing image processing and analysis were a CentOS 7.1 Linux system on a Huawei high-performance cluster computing platform with 12 computing nodes, 240 processor cores, and 250-TB storage capacity in our university.

Statistical Analysis

All statistical analyses were performed using SPSS 24.0 software (IBM Corp.). The two-sample t test and chi-square test were used to analyze age and sex differences between the two groups. In addition, partial correlation coefficients were calculated to evaluate correlations between DKI parameters in abnormal WM regions and the disease duration of HM, using age as a covariate. The statistical threshold was set at 0.05.

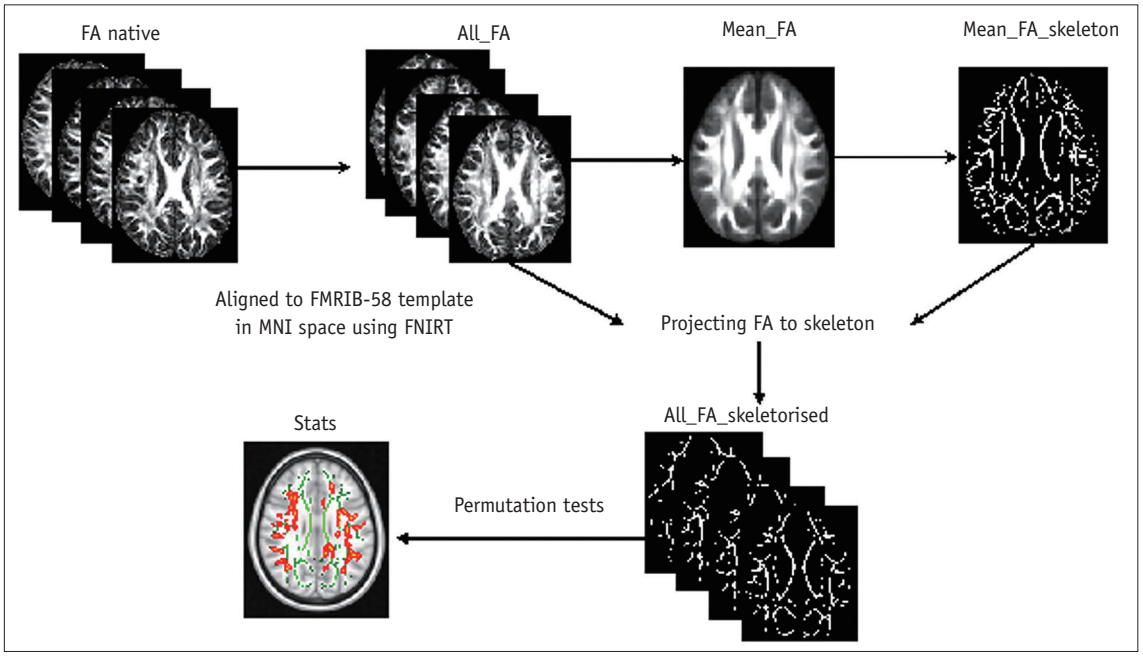

Fig. 1. The processing flow of tract-based spatial statistics analysis. FA = fractional anisotropy, FNIRT = nonlinear registration tool, MNI = Montreal Neurological Institute

https://doi.org/10.3348/kjr.2020.0178

Korean Journal of Radiology
KJR

RESULTS

Demographic and Clinical Characteristics of the Subjects

Thirty patients with HM (age range of 22–65 years, 11 males) and 33 HCs (24–65 years, 14 males) were finally recruited in our study. The baseline data of 63 subjects are shown in Table 1. No significant differences in age or sex were identified between the HM and HC groups (p = 0.315, p = 0.641, respectively).

TBSS Results

Kurtosis Parameters from DKI

Compared to the HCs, the patients with HM had significantly (p < 0.05, two-tailed, TFCE corrected) decreased DKI-derived kurtosis parameters in multiple WM regions, including both WM regions with coherent fiber arrangements, such as the corticospinal tract (CST) and anterior thalamic radiation (ATR), and also WM regions with complex fiber arrangements, such as the superior longitudinal fasciculus (SLF), corona radiata (CR), and juxtacortical WM. AK, RK, MK, and KFA could detect abnormal diffusion in 5.2%, 0.9%, 0.5%, and 0.045% of voxels of the whole WM skeleton, respectively (Fig. 2, Table 2).

Diffusion Parameters Derived from DKI

Compared to the HCs, the HM patients demonstrated significantly (p < 0.05, two-tailed, TFCE corrected) reduced DKI-derived FA and increased DKI-derived AD in WM regions with coherent fiber arrangements, such as the corpus callosum (CC), forceps minor, and CST. No regions showed significantly altered RD or MD. DKI-derived AD and FA could detect abnormal diffusion in 5.2% and 0.9% of voxels of the whole WM skeleton, respectively (Fig. 3, Table 2).

Table 1. Demographic and Clinical Characteristics of HM Patients and HCs

Characteristic	HM Patients (n = 30)	HCs (n = 33)	*P*
Age, years	35.1 ± 13.7	38.6 ± 18.0	0.315*
Sex, female/male	19/11	19/14	0.641†
Duration of illness, years	23.8 ± 11.8	NA	
Refractive diopter_R (D)	-8.4 ± 4	NA	
Refractive diopter_L (D)	-8.5 ± 4	NA	
Axial length_R	28.0 ± 1.7	NA	
Axial length_L	27.9 ± 2.2	NA	

Data are presented as mean ± standard deviation except for sex, for which number of patients is presented. *Two-sample t test, †Chi-squared test. D = diopter, HC = healthy control, HM = high myopia, L = left, NA = not applicable, R = right

Diffusion Changes in Relation to Clinical Measures

Regarding DKI-derived kurtosis parameters, the mean AK values in the left CST (r = -0.379, p = 0.043) and forceps major (r = -0.448, p = 0.015), the mean RK values in the right superior CR (r = -0.421, p = 0.023) and right inferior longitudinal fasciculus (ILF) (r = -0.379, p = 0.042), and the mean MK values in the superior CR (r = -0.376, p = 0.044) and the body of CC (r = -0.430, p = 0.020) all showed significantly negative correlations with disease duration (Fig. 4). Regarding DKI-derived diffusion parameters, the mean AD values in the right ILF (r = 0.372, p = 0.047) and right inferior fronto-occipital fasciculus (IFOF) (r = 0.409, p = 0.028) showed significantly positive correlations with disease duration (Fig. 5).

DISCUSSION

In this study, we used TBSS analysis of DKI data to investigate possible microstructural alterations of brain WM in HM subjects. We observed that compared to HCs, HM patients showed regions with significant reductions in AK, RK, MK, and FA and increases in AD predominately in the bilateral CST, right ILF, SLF, IFOF, and left thalamus. Moreover, correlations were detected between DKI parameters (AK, RK, MK, and AD) in significant brain clusters and disease duration in HM patients.

Major Altered Parameters and Their Clinical Significance

Among the DKI-derived parameters in our study, the most dramatic alterations were observed in AK and AD, which suggested axonal loss. AK, a measure of microstructural complexity along the axial direction of WM fibers, represents the integrity of axons [17]. AD, a metric of diffusion along the long axis, is a biomarker of axonal damage [18]. In our findings, we observed a decrease in AK and an increase in AD primarily in the bilateral CST, left thalamus, right ILF, and right IFOF in the HM group, demonstrating axonal deficits in these fibers. In addition, changes in RK also captured our attention, with affected areas overlapping with some of the regions of altered AK/AD. RK reflects the complexity of the fiber orientation as well as the vertical orientation, and reduced RK has been considered to be specific for demyelination [19]. Therefore, the decrease in RK in HM patients, predominantly in the bilateral CST, left thalamus/ILF, and right ATR/superior CR indicates that

https://doi.org/10.3348/kjr.2020.0178

demyelination is also a pathological alteration caused by HM.

Song et al. [20] examined the optic nerve in a mouse model of retinal ischemia using DTI. They documented that injury to the optic nerve started with axonal degeneration, which was followed by demyelination. In multiple sclerosis (MS) patients, axonal loss has also been considered a principal reason for irreversible neurological disability in multiple studies [21-23]. In line with these viewpoints, we found that certain areas with abnormal RK and AK/AD were

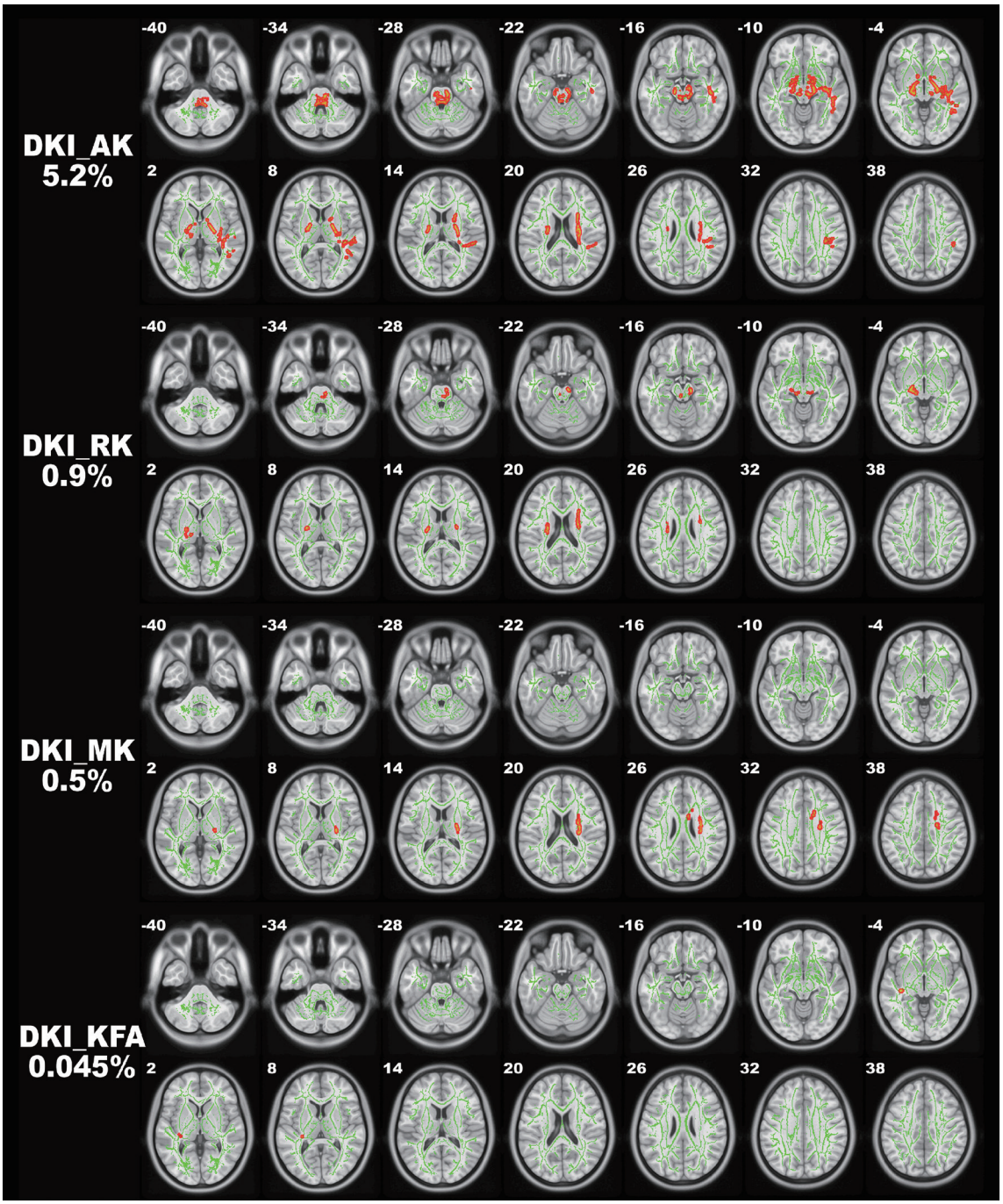

Fig. 2. Comparison of DKI-derived kurtosis parameters between HM patients and HCs. Tract-based spatial statistics shows white matter regions with significant ($p < 0.05$, threshold-free cluster enhancemen corrected) differences in AK, RK, MK, and KFA values between HM patients and HCs. Green represents mean FA skeleton of all participants; red denotes reduction and blue represents increase in HM patients. The percentage in the left column represents the percentage of the abnormal voxels relative to the whole skeleton voxels for each parameter. AK = axial kurtosis, DKI = diffusion kurtosis imaging, FA = fractional anisotropy, HC = healthy control, HM = high myopia, KFA = kurtosis FA, MK = mean kurtosis, RK = radial kurtosis

https://doi.org/10.3348/kjr.2020.0178

Korean Journal of Radiology
KJR

Table 2. Brain Areas with Significantly Different DKI Parameters between the Two Groups (TFCE Corrected)

Skeleton Clusters (> 100 Voxels)	Cluster (Size)	*P*	Peak Voxel MNI Coordinates (mm)		
			x	y	z
HM < HC					
AK					
Right CST	3977	0.006	17	-18	-10
Right ILF	1474	0.021	41	-23	-5
Left thalamus	767	0.013	-17	-24	-2
Left medial globus pallidus/CST	136	0.026	-17	-6	-8
RK					
Left CST/thalamus/ILF	665	0.016	-21	-23	-2
Right CST	243	0.035	12	-22	-17
Right ATR/superior corona radiata	201	0.033	26	5	21
MK					
Right SLF/CST/superior corona radiata	503	0.040	28	-13	26
FA					
Left medial geniculum body/CST	791	0.029	-18	-24	-3
Right CST	404	0.049	29	-9	28
HM > HC					
AD					
Forceps major/Right IFOF	1087	0.037	25	-75	19
Right ILF/IFOF/cingulum (hippocampus)	738	0.039	34	-59	-5
Left CST	591	0.038	-19	-17	-6
Right CST	148	0.047	14	-21	-14

AD = axial diffusivity, AK = axial kurtosis, ATR = anterior thalamic radiation, CST = corticospinal tract, DKI = diffusion kurtosis imaging, FA = fractional anisotropy, HC = healthy control, HM = high myopia, ILF = inferior longitudinal fasciculus, IFOF = inferior fronto-occipital fasciculus, MK = mean kurtosis, MNI = Montreal Neurological Institute, RK = radial kurtosis, SLF = superior longitudinal fasciculus, TFCE = threshold-free cluster enhancemen

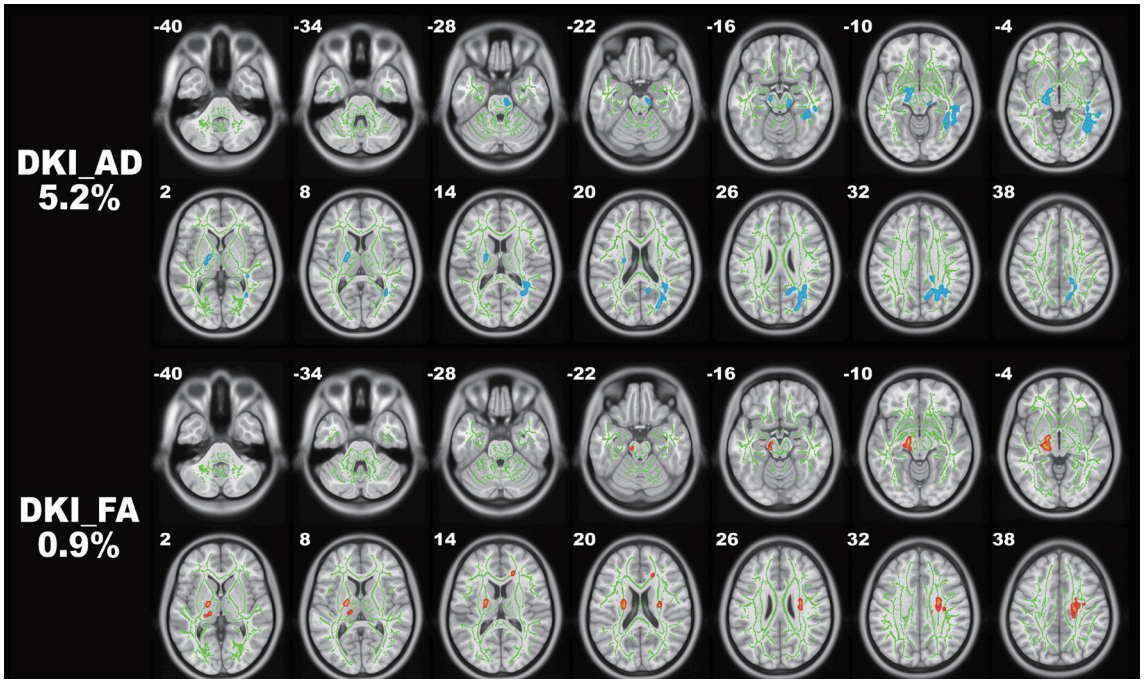

Fig. 3. Comparison of DKI-derived diffusion metrics between HM patients and healthy controls. Tract-based spatial statistics shows white matter regions with significant ($p < 0.05$, threshold-free cluster enhancemen corrected) differences in the DKI-derived FA and AD between HM patients and healthy subjects. Green represents mean FA skeleton of all participants; red denotes reduction and blue represents increase in HM patients. The percentage in the left column represents the percentage of the abnormal voxels relative to the whole skeleton voxels for each parameter. AD = axial diffusivity, DKI = diffusion kurtosis imaging, FA = fractional anisotropy, HM = high myopia

https://doi.org/10.3348/kjr.2020.0178

overlapped in the bilateral CST and left thalamus; however, the cluster sizes of altered AK or AD values were larger than those of altered RK values. In addition, some regions such as the right IFOF and ILF showed AK and AD alterations but without RK alteration. AK and AD were demonstrated to be more sensitive parameters for detecting WM abnormalities in HM. Consequently, we considered that axonal injury may mainly account for the pathogenesis of microstructural damage in HM, similar to the neurodegenerative changes in MS patients [22,23].

To our surprise, FA and MK, the most commonly used metrics of WM integrity, were not sensitive indicators of WM

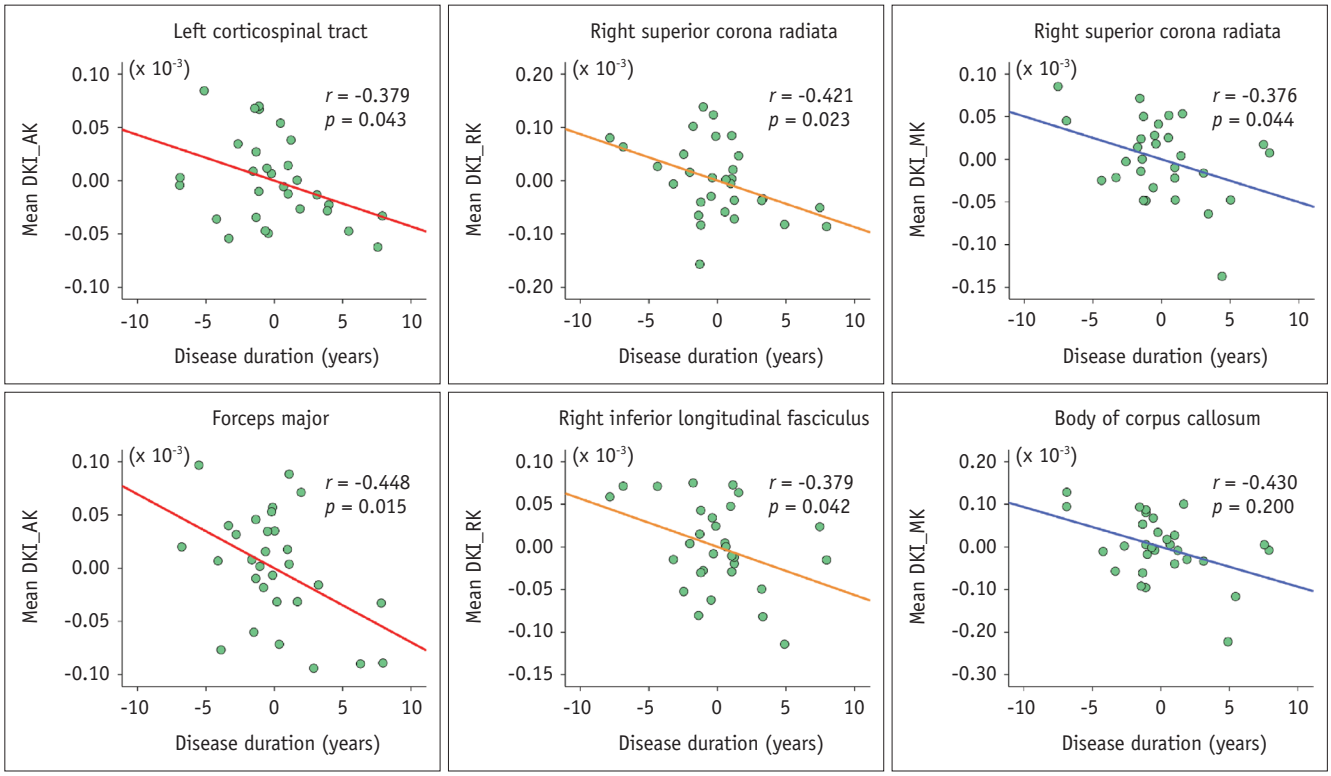

Fig. 4. The Partial correlations of DKI-derived kurtosis parameters (AK, RK, MK) and disease duration. Of note, the coordinate value of both x-axis (disease duration) and y-axis (kurtosis parameter) do not reflect the initial values of these variables, while considering age as a covariate. AK = axial kurtosis, DKI = diffusion kurtosis imaging, MK = mean kurtosis, RK = radial kurtosis

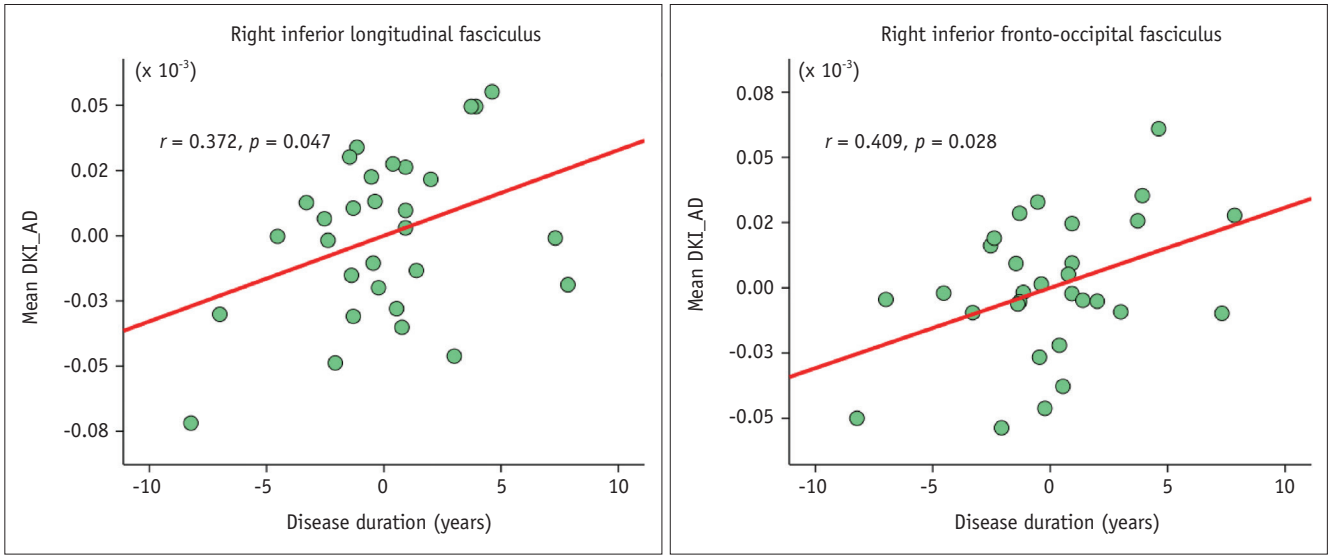

Fig. 5. The partial correlations of DKI-derived diffusion parameter (AD) and disease duration, using age as a covariate. AD = axial diffusivity, DKI = diffusion kurtosis imaging

https://doi.org/10.3348/kjr.2020.0178

Korean Journal of Radiology
KJR

damage in our study. FA measures the degree of anisotropy of water molecules and can indicate decreased WM integrity caused by demyelination and axonal degradation [24,25]. FA is suitable for assessing WM with coherent fiber arrangements, such as the CST, but has a limited ability to evaluate WM integrity in regions with crossing fibers, such as the SLF and ILF. In our study, multiple complex fiber arrangement alterations were noted, which may explain why FA was not very sensitive in detecting WM injury in HM patients. MK represents the average kurtosis along all diffusion gradient-encoding directions; however, kurtosis alterations predominantly occurred in the axial direction, and the MK in all orientations was not notably significant, which may be why the change in MK in our study was not remarkable.

Changes in Neural Bundles

In the current study, microstructural impairments in the HM patients mainly occurred in the bilateral CST, right ILF, SLF, IFOF, and left thalamus. The CST is an important motor conduction bundle and is critically important for motion control [26]. The CST abnormalities detected by DKI in HM patients indicate motor conduction dysfunction. Previous studies have reported that the deafferentation of relevant sensory input neurons may affect the integrity of WM in the brain [27]. Microstructural injury of the CST was found in patients with congenital and late-onset blindness [27], patients with optic neuropathy [28], and hyperopic children with reduced near visual function [29], demonstrating that abnormal visual information input may cause motor conduction dysfunction. In line with these studies, the patients with HM in our study also exhibited microstructural impairments in CST.

The ILF, SLF, and IFOF are pathways for higher visual processes [30-32]. The ILF bundle has vital roles in the rapid transfer of visual information [33,34], object recognition [35], and visual memory [36]. The SLF is the primary direct pathway relating to visuospatial attention [30,37], and the IFOF provides neurological signals for visual processing [38] and facial emotion recognition [39]. The literature reflects a consensus that the integrity of the ILF, SLF, and IFOF has remarkable associations with visual functions, especially higher visual processing [26,37,40]. Abnormal fiber bundles related to visual processes have also been found in previous research. Kang et al. [41] analyzed neural changes in a later phase of visual perceptual learning and detected altered FA in the ILF. A study of long-term video game players, who need superior visual skills, showed higher WM integrity in the higher-tier visual pathways [26].

In addition, the thalamus is widely known to play a crucial role in providing wide-ranging connectivity to manage visual, auditory, and somatosensory input information [42,43]. Moreover, significant atrophy in the left geniculate nucleus, which is located in the thalamus, has been found in glaucoma patients [44]. The microstructural alterations observed in our study were mainly detected in the CST, ILF, SLF, IFOF, and thalamus, reminding us that HM seems to have intimate associations with deficits in motor conduction and higher visual processing.

Correlations between Imaging Parameters and Clinical Variables

The relationships between diffusion eigenvalues in abnormal WM fiber tracts and clinical measures were analyzed. Among kurtosis parameters, the mean AK values in the left CST and forceps major, the mean RK values in the right superior CR and ILF, and the mean MK values in the superior CR and the body of CC showed significantly negative correlations with disease duration. The mean AD values in the right ILF and IFOF showed significantly positive correlations with disease duration, among diffusion parameters. Thus, HM progression can be assumed to correspond to lower kurtosis parameters, higher diffusion metrics, and more serious WM damage. Therefore, our results regarding the correlations between changes in DKI-derived parameters and disease duration suggest that DKI is a sensitive tool for detecting microstructural injury in WM tracts and can provide meaningful information for detecting microstructural injury and monitoring disease progression.

Limitations

The limitations of this article should also be noted: 1) We focused only on the capacity of DKI to detect WM abnormality using the TBSS method and advanced data processing, which require thinner slice thickness and more independent diffusion gradient directions to yield more information on brain alterations, such as neurite orientation dispersion and density imaging; 2) Information on educational levels and family history of the disease was not collected, which may affect our results; 3) Some elderly subjects, who may have had WM degeneration, were included in our study. However, we ensured that the subjects in the two groups were age-matched; therefore,

 https://doi.org/10.3348/kjr.2020.0178

we are confident that age had little effect on the present results; 4) The pathophysiology of HM and associated WM alterations may be different in patients of different ages, and grouping subjects by age may lead to more robust results. Therefore, we will expand the sample size in further research and stratify subjects according to age.

In summary, our TBSS analysis of DKI data revealed microstructural abnormalities in HM subjects predominantly in the bilateral CST, right ILF, SLF, IFOF, and left thalamus. DKI is a promising tool for detecting microstructural damage in HM, which may be helpful for exploring and monitoring the pathogenesis of the disease.

Conflicts of Interest

The authors have no potential conflicts of interest to disclose.

Author Contributions

Conceptualization: Huihui Wang. Data curation: Huihui Wang, Zhenchang Wang. Formal analysis: Huihui Wang, Hongwei Wen. Funding acquisition: Jing Li, Zhenchang Wang. Investigation: Huihui Wang, Hongwei Wen. Methodology: Huihui Wang, Hongwei Wen, Zhenchang Wang. Project administration: Huihui Wang, Zhenchang Wang. Resources: Huihui Wang, Shanshan Li, Yanling Wang, Zhenchang Wang. Software: Huihui Wang, Hongwei Wen, Qian Chen, Zhenchang Wang. Supervision: Zhenchang Wang. Validation: Zhenchang Wang. Visualization: Huihui Wang, Zhenchang Wang. Writing—original draft: Huihui Wang. Writing—review & editing: Huihui Wang, Zhenchang Wang.

ORCID iDs

Huihui Wang
https://orcid.org/0000-0001-7908-8030
Hongwei Wen
https://orcid.org/0000-0003-1717-7235
Jing Li
https://orcid.org/0000-0001-9392-6600
Qian Chen
https://orcid.org/0000-0001-5210-9647
Shanshan Li
https://orcid.org/0000-0002-5905-5247
Yanling Wang
https://orcid.org/0000-0002-3487-0122
Zhenchang Wang
https://orcid.org/0000-0001-8190-6469

REFERENCES

1. Holden BA, Wilson DA, Jong M, Sankaridurg P, Fricke TR, Smith EL III, et al. Myopia: a growing global problem with sight-threatening complications. *Community Eye Health* 2015;28:35
2. Morgan IG, French AN, Ashby RS, Guo X, Ding X, He M, et al. The epidemics of myopia: aetiology and prevention. *Prog Retin Eye Res* 2018;62:134-149
3. Hsu CC, Chen SJ, Li AF, Lee FL. Systolic blood pressure, choroidal thickness, and axial length in patients with myopic maculopathy. *J Chin Med Assoc* 2014;77:487-491
4. Morgan IG, Ohno-Matsui K, Saw SM. Myopia. *Lancet* 2012;379:1739-1748
5. Huang X, Hu Y, Zhou F, Xu X, Wu Y, Jay R, et al. Altered whole-brain gray matter volume in high myopia patients: a voxel-based morphometry study. *Neuroreport* 2018;29:760-767
6. Li Q, Guo M, Dong H, Zhang Y, Fu Y, Yin X. Voxel-based analysis of regional gray and white matter concentration in high myopia. *Vision Res* 2012;58:45-50
7. Shu N, Li J, Li K, Yu C, Jiang T. Abnormal diffusion of cerebral white matter in early blindness. *Hum Brain Mapp* 2009;30:220-227
8. Marcus MW, de Vries MM, Junoy Montolio FG, Jansonius NM. Myopia as a risk factor for open-angle glaucoma: a systematic review and meta-analysis. *Ophthalmology* 2011;118:1989-1994.e2
9. Xu ZF, Sun JS, Zhang XH, Feng YY, Pan AZ, Gao MY, et al. Microstructural visual pathway abnormalities in patients with primary glaucoma: 3 T diffusion kurtosis imaging study. *Clin Radiol* 2018;73:591.e9-591.e15
10. Allen B, Schmitt MA, Kushner BJ, Rokers B. Retinothalamic white matter abnormalities in amblyopia. *Invest Ophthalmol Vis Sci* 2018;59:921-929
11. Basser PJ, Jones DK. Diffusion-tensor MRI: theory, experimental design and data analysis - a technical review. *NMR Biomed* 2002;15:456-467
12. Veraart J, Poot DH, Van Hecke W, Blockx I, Van der Linden A, Verhoye M, et al. More accurate estimation of diffusion tensor parameters using diffusion kurtosis imaging. *Magn Reson Med* 2011;65:138-145
13. Zhu J, Zhuo C, Qin W, Wang D, Ma X, Zhou Y, et al. Performances of diffusion kurtosis imaging and diffusion tensor imaging in detecting white matter abnormality in schizophrenia. *Neuroimage Clin* 2015;7:170-176
14. Tabesh A, Jensen JH, Ardekani BA, Helpern JA. Estimation of tensors and tensor-derived measures in diffusional kurtosis imaging. *Magn Reson Med* 2011;65:823-836
15. Wen H, Liu Y, Wang J, Rekik I, Zhang J, Zhang Y, et al. Combining tract-and atlas-based analysis reveals microstructural abnormalities in early tourette syndrome children. *Hum Brain Mapp* 2016;37:1903-1919
16. Smith SM, Jenkinson M, Johansen-Berg H, Rueckert D, Nichols TE, Mackay CE, et al. Tract-based spatial statistics:

https://doi.org/10.3348/kjr.2020.0178

voxelwise analysis of multi-subject diffusion data. *Neuroimage* 2006;31:1487-1505
17. Wu EX, Cheung MM. MR diffusion kurtosis imaging for neural tissue characterization. *NMR Biomed* 2010;23:836-848
18. Wang R, Tang Z, Sun X, Wu L, Wang J, Zhong Y, et al. White matter abnormalities and correlation with severity in normal tension glaucoma: a whole brain atlas-based diffusion tensor study. *Invest Ophthalmol Vis Sci* 2018;59:1313-1322
19. Falangola MF, Guilfoyle DN, Tabesh A, Hui ES, Nie X, Jensen JH, et al. Histological correlation of diffusional kurtosis and white matter modeling metrics in cuprizone-induced corpus callosum demyelination. *NMR Biomed* 2014;27:948-957
20. Song SK, Sun SW, Ju WK, Lin SJ, Cross AH, Neufeld AH. Diffusion tensor imaging detects and differentiates axon and myelin degeneration in mouse optic nerve after retinal ischemia. *Neuroimage* 2003;20:1714-1722
21. van der Valk P, De Groot CJ. Staging of multiple sclerosis (MS) lesions: pathology of the time frame of MS. *Neuropathol Appl Neurobiol* 2000;26:2-10
22. De Stefano N, Narayanan S, Francis GS, Arnaoutelis R, Tartaglia MC, Antel JP, et al. Evidence of axonal damage in the early stages of multiple sclerosis and its relevance to disability. *Arch Neurol* 2001;58:65-70
23. Phillips J. Rethinking multiple sclerosis. *Arch Neurol* 2001;58:30-32
24. Glenn GR, Helpern JA, Tabesh A, Jensen JH. Quantitative assessment of diffusional kurtosis anisotropy. *NMR Biomed* 2015;28:448-459
25. Douaud G, Jbabdi S, Behrens TE, Menke RA, Gass A, Monsch AU, et al. DTI measures in crossing-fibre areas: increased diffusion anisotropy reveals early white matter alteration in MCI and mild alzheimer's disease. *Neuroimage* 2011;55:880-890
26. Zhang Y, Du G, Yang Y, Qin W, Li X, Zhang Q. Corrigendum: higher integrity of the motor and visual pathways in long-term video game players. *Front Hum Neurosci* 2015;9:98
27. Wang D, Qin W, Liu Y, Zhang Y, Jiang T, Yu C. Altered white matter integrity in the congenital and late blind people. *Neural Plast* 2013;2013:128236
28. Long M, Wang L, Tian Q, Ding H, Qin W, Shi D, et al. Brain white matter changes in asymptomatic carriers of Leber's hereditary optic neuropathy. *J Neurol* 2019;266:1474-1480
29. Lundberg K, Suhr Thykjaer A, Søgaard Hansen R, Vestergaard AH, Jacobsen N, Goldschmidt E, et al. Physical activity and myopia in danish children-the CHAMPS eye study. *Acta Ophthalmol* 2018;96:134-141
30. Parks EL, Madden DJ. Brain connectivity and visual attention. *Brain Connect* 2013;3:317-338
31. Chechlacz M, Rotshtein P, Hansen PC, Riddoch JM, Deb S, Humphreys GW. The Neural underpinings of simultanagnosia: disconnecting the visuospatial attention network. *J Cogn Neurosci* 2012;24:718-735
32. Klarborg B, Skak Madsen K, Vestergaard M, Skimminge A, Jernigan TL, Baaré WF. Sustained attention is associated with right superior longitudinal fasciculus and superior parietal white matter microstructure in children. *Hum Brain Mapp* 2013;34:3216-3232
33. Catani M, Jones DK, Donato R, Ffytche DH. Occipito-temporal connections in the human brain. *Brain* 2003;126:2093-2107
34. Catani M, Thiebaut de Schotten M. A diffusion tensor imaging tractography atlas for virtual in vivo dissections. *Cortex* 2008;44:1105-1132
35. Shin J, Rowley J, Chowdhury R, Jolicoeur P, Klein D, Grova C, et al. Inferior longitudinal fasciculus' role in visual processing and language comprehension: a combined MEG-DTI study. *Front Neurosci* 2019;13:875
36. Ross ED. Sensory-specific amnesia and hypoemotionality in humans and monkeys: gateway for developing a hodology of memory. *Cortex* 2008;44:1010-1022
37. Umarova RM, Saur D, Schnell S, Kaller CP, Vry MS, Glauche V, et al. Structural connectivity for visuospatial attention: significance of ventral pathways. *Cereb Cortex* 2010;20:121-129
38. Fox CJ, Iaria G, Barton JJ. Disconnection in prosopagnosia and face processing. *Cortex* 2008;44:996-1009
39. Philippi CL, Mehta S, Grabowski T, Adolphs R, Rudrauf D. Damage to association fiber tracts impairs recognition of the facial expression of emotion. *J Neurosci* 2009;29:15089-15099
40. Mayer KM, Vuong QC. TBSS and probabilistic tractography reveal white matter connections for attention to object features. *Brain Struct Funct* 2014;219:2159-2171
41. Kang DW, Kim D, Chang LH, Kim YH, Takahashi E, Cain MS, et al. Structural and functional connectivity changes beyond visual cortex in a later phase of visual perceptual learning. *Sci Rep* 2018;8:5186
42. Phillips JW, Schulmann A, Hara E, Winnubst J, Liu C, Valakh V, et al. A repeated molecular architecture across thalamic pathways. *Nat Neurosci* 2019;22:1925-1935
43. Van Cauter S, Veraart J, Sijbers J, Peeters RR, Himmelreich U, De Keyzer F, et al. Gliomas: diffusion kurtosis MR imaging in grading. *Radiology* 2012;263:492-501
44. Lu P, Shi L, Du H, Xie B, Li C, Li S, et al. Reduced white matter integrity in primary open-angle glaucoma: a DTI study using tract-based spatial statistics. *J Neuroradiol* 2013;40:89-93

 https://doi.org/10.3348/kjr.2020.0178